Numerical simulation of seawater intrusion in the lower Seybouse aquifer system, Algeria

Simulazione numerica del fenomeno di intrusione salina nel sistema acquifero di Seybouse, Algeria

Samir HANI[a], Fayçal TOUMI[a] ✉ , Nabil BOUGHERIRA[a], Isam SHAHROUR[b], Azzedine HANI[a]

[a] Water Resources and Sustainable Development Laboratory (REDD). Badji Mokhtar Annaba University

email ✉ : *faycaltoumi@hotmail.com*; email: *Hani.samir@outlook.fr; nabilbough@gmail.com; haniazzedine@yahoo.fr*

[b] Civil Engineering and Geo Environment Laboratory (LGCgE). University of Lille, 59650 Villeneuve d'Ascqcedex, France
email: *isam.shahrour@univ-lille1.fr*

Correspondence to:
Fayçal Toumi ✉
faycaltoumi@hotmail.com

Riassunto

Il fenomeno dell'intrusione salina rappresenta un fattore di rischio per l'approvvigionamento idrico, l'agricoltura e le attività industriali nella regione di Seybouse, nel nord-est dell'Algeria. Per analizzare questo rischio, è stato sviluppato un modello tridimensionale utilizzando i codici MODFLOW ed MT3DMS per prevedere gli effetti dell'intrusione salina sull'acquifero costiero. L'applicazione di questo modello indica che i prelievi di acque sotterranee determinano un continuo abbassamento del livello idrico e un aumento della concentrazione di cloruri. Inoltre, il fronte salino potrebbe avanzare da 300 a 2500 m verso l'entroterra. Questi risultati mostrano la necessità di misure adeguate per la protezione dell'acquifero. Le previsioni numeriche per il 2045, considerando un aumento dei prelievi di falda del 20%, mostrano una diminuzione importante dei livelli idrici, fino a -6 m rispetto al livello medio del mare, e un aumento delle concentrazioni di Cl⁻ fino a circa 10 km nell'entroterra .

Abstract

Seawater intrusion represents a high risk for the water supply, the agriculture and industry activities in the lower Seybouse region of North-Eastern Algeria. In order to analyze this risk, a three-dimensional model was developed using the MODFLOW and MT3DMS codes to predict seawater intrusion in the coastal aquifer. The application of this model indicates that the groundwater withdrawals result in a continuous decrease of the water level and in an increase of chloride concentration. Moreover, the salt front could progress by 300 to 2500 m in the land. These results show the necessity of adequate measures for the protection of the aquifer. Numerical predictions for 2045, considering an increase of groundwater withdrawals by 20%, show a fairly significant decrease in water levels, up to -6 m with respect to the mean sea level, and an increase of Cl⁻ concentrations up to about 10 km inland.

Introduction

Fresh groundwater resources in coastal aquifers are significantly impacted by seawater intrusion (Chang & Yeh, 2010; Mastrocicco, 2021). Climate change, sea level rise, change in land use and excessive groundwater pumping led to severe seawater intrusion (Yang et al., 2013). Coastal areas are the most populated regions in the world (Werner et al., 2013). The public water supply, together with the agriculture and industry activities, resulted in an important overexploitation of the coastal aquifers (Datta et al., 2009) and consequently to seawater intrusion which damaged the coastal groundwater resources (Ilias & Pericles, 2016).

Prediction of the seawater intrusion requires a multidisciplinary approach (Yang et al., 2013; Werner et al., 2013; Datta et al., 2009; Sappa et al., 2017; Sappa et al., 2019; Alfio et al., 2020; Sae-Ju et al., 2020).

Several authors (Oude Essink, 2001; Comte, 2008; Cimino et al., 2008) used analytical, geophysical and numerical methods to determine the position of the interface between freshwater and marine water. Other authors (Alfio et al., 2022; Acuña-Alonso et al., 2021; Sappa et al., 2019; Bouderbala, 2015) analyzed the chemical processes and reactions responsible for the enrichment or depletion of the groundwater with chemical elements. Several approaches were used to study marine intrusion (Yang et al., 2013; Werner et al., 2013; Datta et al., 2009; Parisi et al. 2022) with emphasis on:

– the role of the major hydrodynamic factors;
– the analysis of the sources and origins of salinization;
– the correlation between the major elements concentrations and the Cl^- ion concentration, which constitutes a good salinity tracer;
– the development of a numerical model of pollutant transport.

This paper presents an analysis of the saltwater intrusion in the coastal plain of Annaba using the MODFLOW code (Harbaugh, 2005) coupled to the MT3DMS model (Zheng et al., 2012).

MODFLOW allowed to analyze the effects of the intensification of pumping rates in the plain on the aquifer. Steady-state calibration of the model was used to check the boundary conditions assumptions. Transient simulations allowed to improve knowledge about the distribution of the aquifer storage coefficients and to analyze the hydrodynamic evolution of the aquifer.

The use of the MT3DMS model involved calibrating the salinity of the groundwater (expressed as Cl^- concentration) in steady-state and then in transient conditions over a period of 12 years.

Materials and Methods
Study Area

The studied area is located in the extreme North Eastern part of Algeria. It is bounded to the North by the Mediterranean Sea, to the West by the metamorphic Edough complex, to the South by the Fetzara Lake and by the Numidian chain of Cheffia mounts (Fig. 1). The aquifer formation is composed of Mio-Pliocene and Quaternary sediments of the Ben-Ahmed graben. Such formation is composed of an alternation of clays, sandy clays, sands and gravels. Two main aquifers can be distinguished (Fig. 2):

– The **unconfined superficial aquifer**, which is located in sandy-clayey formations, including sandy lenses, with a transmissivity of this horizon varies from between $2 \cdot 10^{-6}$ and $8 \cdot 10^{-5}$ m²/s. Despite its low hydrodynamic potential, this aquifer feeds, by leakage, the main gravel and pebble aquifer below.
– The **confined deep aquifer**, which is located in an alternation of coarse layers of gravel and pebbles and clayey-sandy layers. Its transmissivity varies from 10^{-4} to 10^{-2} m²/s with a storage coefficient varying between 10^{-4} and 10^{-3}.

These two aquifers are generally separated by a semi-permeable horizon consisting of sandy clay, silt, clay and sand. The thickness of this layer varies from 0 m in the Southern and Western borders to more than 75 m in the coastal part. The permeability of the semi-permeable horizon varies from 10^{-8} to 10^{-7} m/s.

Previous studies (Lamouroux & Hani, 2006; Majour et al., 2018) in the Seybouse region pointed out the following:

– a decrease in the water levels occurred from 1995 to 2009, due to the intensive use of groundwater near the coast (Fig. 3);
– the dip of the gravel strata mainly occurs towards the sea: the geometrical characteristics (thickness and dip changes) of the gravel layer shows that the deep aquifer sediments outcrop few kilometers (about 4-5 km) from the coast (Vila, 1980).
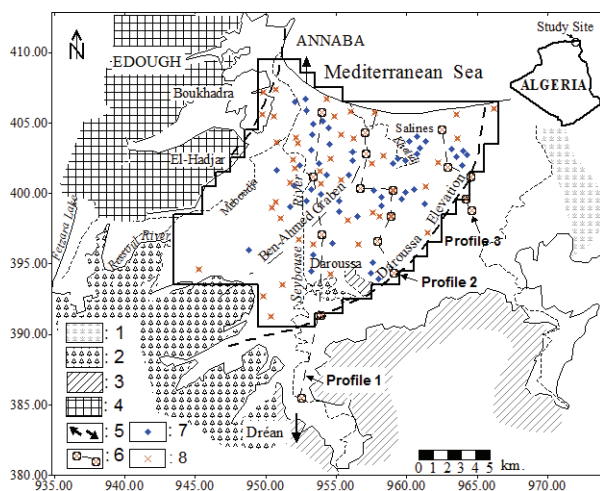

Fig. 1 - *Location map of the study area. 1. Marshes, 2. Ancient Alluvium, 3. Numidian sandstone or clay, 4. Metamorphic formation, 5. Cross Section S-N, 6. Physico-chemical Profiles, 7. Pumping Well, 8. Monitoring network.*

Fig. 1 - Ubicazione dell'area di studio. 1. Paludi, 2. Sedimenti alluvionali, 3. Arenaria o argilla Numidiana, 4. Formazione metamorfica, 5. Sezione S-N, 6. Profili dei parametri chimico-fisici, 7. Pozzo di emungimento, 8. Rete di monitoraggio.
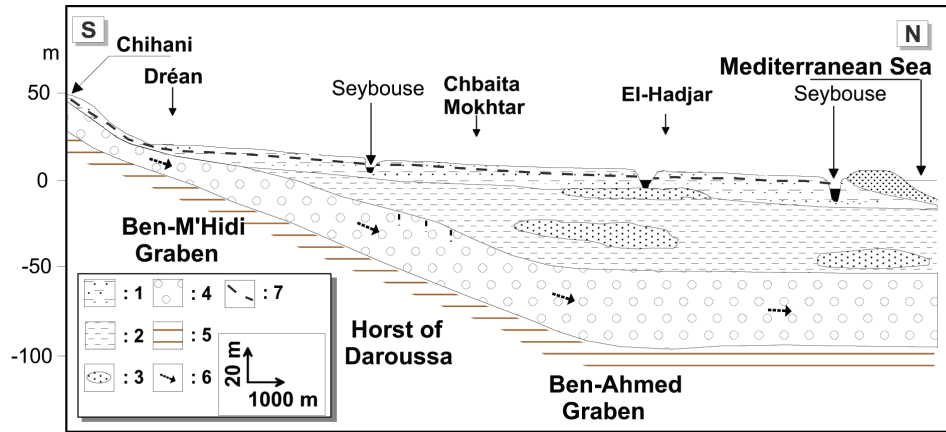
Fig. 2 - *Cross section S-N through the lower Seybouse aquifer system (the profile of the cross section can be inferred from the item 5 in Fig.1). 1. Sandy-clayey formations including sand lenses (superficial aquifer), 2. Sandy clay, silt, clay and sand (semi-permeable horizon), 3. Sands, 4. Alternation of coarse layers of gravel and pebbles and clayey-sandy layers (deep gravel layer), 5. Numidian or Paleocene clays; 6. Groundwater level of the deep aquifer, 7. Direction of flow in the deep aquifer. Elevation is expressed in m with respect to the mean sea level.*

Fig. 2 - Sezione S-N attraverso il sistema acquifero di Seybouse (il profilo della sezione è indicato dall'elemento 5 in Fig.1). 1. Formazioni sabbioso-argillose con lenti sabbiose (acquifero superficiale), 2. Sabbie argillose, limi, argille e sabbie (orizzonte semi-permeabile), 3. Sabbie, 4. Alternanza tra strati grossolani di ghiaie e ciottoli e strati argilloso-sabbiosi (strato ghiaioso profondo), 5. Argille Numidiane Paleoceniche; 6. Livello dell'acquifero profondo, 7. Direzione di flusso dell'acquifero profondo. Le quote sono espresse in m rispetto al livello medio del mare.
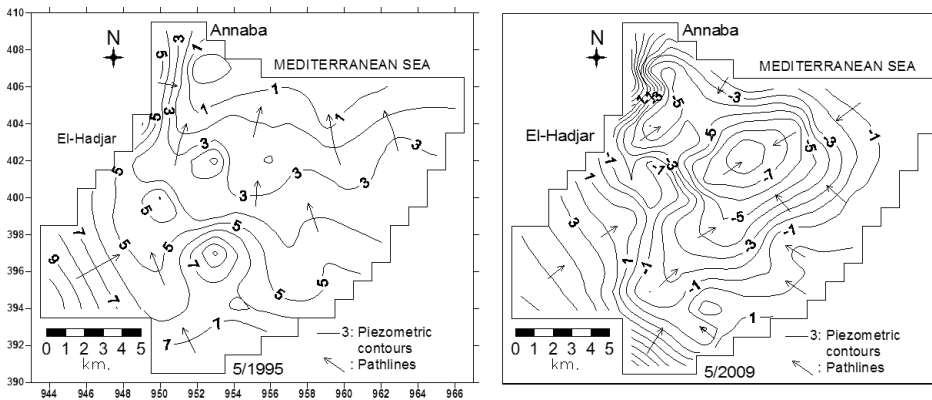

Fig. 3 - *Variation of piezometric levels between 1995 and 2009 (values in m above mean sea level).*

Fig. 3 - Variazione del livello dell'acquifero tra il 1995 e il 2009 (valori in m sul livello medio del mare).

Piezometric level measurements and geochemical analysis were carried out in 2009-2012 over a network of 45 water points in the deep Seybouse gravel aquifer.

Electrical conductivity (EC) was measured using a WTW multiparameter (Multiline P3 PH/LF SET). Chloride and sodium concentrations were determined by the volumetric method (AFNOR, 1987). The strontium contents were measured by ICP-MS with an accuracy of 5%. Results are presented in section *"Evolution of the groundwater mineralization as a function of distance to the sea"*.

The collected data was used in the groundwater flow and mass transport model for the assessment of the impact of abstractions on the Seybouse coastal aquifer (sections *"Groundwater flow model"* and *"Simulation of saltwater intrusion"*).

Methodology

Two approaches have been used to study the impact of the water withdrawals on the Seybouse coastal aquifer:
1. analysis of the piezometric and physico-chemical measurements of the gravel aquifer, which constitutes the main water resource in the region. The needed data was provided by the National Agency for Water Resources (ANRH) through unpublished documents. Unfortunately, the measurements were not carried out regularly at the same points, due to difficulties in accessing water points, influence of pumping around the piezometers, etc…;
2. development of a groundwater flow and transport model.

The hydraulic head (h) is obtained from the solution of a three-dimensional groundwater flow equation (Bear, 1972):

$$\frac{\partial}{\partial \chi_i}\left[K_{ii}\frac{\partial h}{\partial \chi_i} \right] + q_s = S_s \frac{\partial h}{\partial t} \qquad (1)$$

where:
- t is time (T);
- X_i is the distance along the respective Cartesian coordinate axis (L);
- K is the hydraulic conductivity of the porous material (L/T);
- S_s is the specific storage of the porous material (L^{-1});
- q_s is the source/sink term (T^{-1}).

The transport equation is linked to the flow equation through groundwater velocity term given by:

$$v_i = \frac{K_{ii}}{\theta} \frac{\partial h}{\partial \chi_i} \qquad (2)$$

where:
- K_{ii} is the principal component of the hydraulic conductivity tensor (L/T);
- θ is the porosity of the porous medium.

The partial differential equation describing three-dimensional transport of contaminants in groundwater (Javandel le Pape et al., 1984) can be written as:

$$\frac{\partial C}{\partial t} = \frac{\partial}{\partial \chi_i}\left[D_{ij}\frac{\partial C}{\partial \chi_i} \right] - \frac{\partial}{\partial \chi_i}(v_i C) + \frac{q_s}{\theta}C_s + \sum_{K=1}^{N} R_k \qquad (3)$$

where:
- C is the concentration of contaminants dissolved in groundwater (M/L^3);
- t is time (T);
- χ_i is the distance along the respective Cartesian coordinate axis (L);
- D_{ij} is the hydrodynamic dispersion coefficient (L^2/T);
- v_i is the seepage or linear pore water velocity (L/T);
- q_s is the volumetric flux of water per unit volume of aquifer representing sources (positive) or sinks (negative) (1/T);
- C_s is the concentration of the sources or sinks (M/L^3);
- θ is the porosity of the porous medium;
- Rk is the chemical reaction term [M/(L^{3}T)].

Assuming that only equilibrium controlled linear or non-linear sorption and first order irreversible rate reactions are involved in the chemical reactions. The chemical reaction term can be expressed as (Grove & Stollenwerk, 1984):

$$\sum_{K=1}^{N} R_k = \frac{\rho_b}{\theta}\frac{\partial \overline{C}}{\partial t} - \lambda\left[C + \frac{\rho}{\theta}\overline{C} \right] \qquad (4)$$

where:
- $\overline{C}$ is the concentration of contaminants sorbed on the porous medium;
- λ is the first-order reaction rate (1/T);
- ρ_b is the bulk density of the porous medium (M/L^3).

Rewriting the first term on the right side of Equation (4) as:

$$\frac{\rho_b}{\theta}\frac{\partial \overline{C}}{\partial t} = \frac{\rho_b}{\theta}\frac{\partial C}{\partial t}\frac{\partial \overline{C}}{\partial C} \qquad (5)$$

Equation (3) can be rewritten by substituting Equations (4) and (5) as:

$$\frac{\partial C}{\partial t} = \frac{\partial}{\partial \chi_i}\left[D_{ij}\frac{\partial C}{\partial \chi_j} \right] - \frac{\partial}{\partial \chi_i}(v_i C) + \frac{q_s}{\theta}C_s - \frac{\rho_b}{\theta}\frac{\partial C}{\partial t}\frac{\partial \overline{C}}{\partial C} - \lambda\left(C + \frac{\rho_b}{\theta}\overline{C} \right) \qquad (6)$$

Rearranging the terms, the governing equation of mass transport model is obtained:

$$R\frac{\partial C}{\partial t} = \frac{\partial}{\partial \chi_i}\left[D_{ij}\frac{\partial C}{\partial \chi_j} \right] - \frac{\partial}{\partial \chi_i}(v_i C) + \frac{q_s}{\theta}C_s - \lambda\left(C + \frac{\rho_b}{\theta}\overline{C} \right) \qquad (7)$$

Where R is the retardation factor, defined as:

$$R = 1 + \frac{\rho_b}{\theta}\frac{\partial \overline{C}}{\partial C} \qquad (8)$$

In this paper, the MODFLOW software (Harbaugh, 2005) was used to analyze the effects of withdrawals on the Seybouse coastal aquifer system. The modeled area extends for 264 km^2. It was discretized horizontally into 1056 square cells of 500 m side and vertically into four layers representing the superficial aquifer, the semi-permeable horizon, the deep gravel aquifer and the Numidian clay bedrock. The elevations of the ground surface and of the bottoms of each horizon were determined from the analysis of the available drilling data.

The permeabilities of each layer were determined using the transmissivity values resulting from the available pumping tests carried out in the region.

Effective rainfall was calculated by the Thornthwaite's formula using monthly rainfall and temperatures observed at Salines station over a 32 years period (1985 to 2017).

The main rivers of the region were represented through the River MODFLOW package (Harbaugh, 2005), using the gauging carried out by the National Agency for Water Resources upstream of the plain.

The superficial aquifer is limited to the North, along the coast, by the dune cord, which contains an aquifer with a higher water level, having the effect of blocking groundwater flow towards the sea and creating swamps. The Western limit is made up of the old Edough massifs (micaschists and gneisses), whose altered parts contain an untapped low permeability aquifer. South of the Western border, the isopiezes show a very low influx of water from Lake Fetzara. To the South and East, along the boundary with the horst of Daroussa, the piezometric maps show continuity of the aquifer, which suggests permanent exchanges with the rest of the plain. The inflow to the superficial horizon is ensured by the infiltration of rainwater and runoff from the Seybouse and Meboudja rivers. The outflows from the aquifer are related to the drainage of surface water and to evaporation.

The gravel deep aquifer is limited to the North by the Mediterranean Sea, which is its main outlet. To the West, the aquifer receives a weak supply from metamorphic limestones and alluvium from the high terraces.

As far as the Eastern limit is concerned, two hypotheses can be envisaged. Given the thinning of the gravel levels, in this sector, bordered by the Ben-Ahmed graben, where the piezometry indicates a continuity of flows over the whole of the plain. This limit can be assimilated either to a barrier boundary or to a permeable boundary. The validity of these hypotheses were tested numerically during the calibration of the model.

To the South, in the Dréan sector, the aquifer, which is less than 10 m deep, receives inputs from rainfall recharge, the Seybouse River and underground inputs from the alluvium of the high terraces.

The MODFLOW code was coupled to the MT3DMS model (Zheng & Wang, 1999) for the following scopes: i) simulation of saltwater intrusion stabilization up to 2003, ii) simulation of the evolution of salinity from 2003 to 2015, integrating hydroclimatic data acquired during this period and iii) 30-years forecast simulation of salinity from 2015 to 2045.

To simulate the mineral load of the Mediterranean Sea, a chloride concentration (Cl⁻) of 25 g/L was imposed at the Northern limit, based on the analysis of samples of seawater periodically collected during the campaigns carried out on the wells of the plain. In addition, a longitudinal dispersion value varying from 10 to 20 m and a porosity of 20% were applied to all the cells of the model. The transverse dispersion was fixed between 0.1 and 0.2 m (INERIS, 2000).

Simulation of saltwater intrusion is affected by uncertainties related to (Lucassou et al., 2019):

– the conceptual groundwater flow model: all the characteristics of the freshwater flow model (geometry, boundary conditions, hydrodynamic parameters, in particular permeability and storage coefficient, etc.) will have a preponderant influence on the validity of the results in terms of salinity;

– incorrect initialization of the salinity distribution: the salinity measurements used in the calibration phase

must correspond to a stabilized hydrodynamic state of the aquifer with a freshwater-saltwater balance invariant in time (pseudo-permanent regime). This is a major source of error in the case of heavily exploited aquifers, because the hydrodynamic rebalancing that manifests itself in a more or less marked displacement of the freshwater-saltwater interface can last several years. This rebalancing may never be achieved with time-varying sampling flows;

– numerical dispersion: the transport and mixing effects in modelling processes generates non-linearities in transport equations and numerical oscillations that can lead to calculation errors and/or non-convergence problems.

In this study, the TVD resolution method (third-order method) was adopted to minimize the numerical dispersions and oscillations related to the advection and dispersion effects (Zouhri et al., 2009).

Results and Discussion
Evolution of the groundwater mineralization as a function of distance to the sea

To highlight the influence of the saltwater intrusion on the groundwater quality, we present here the spatial distribution of chlorides Cl⁻, sodium Na⁺, strontium Sr contents and the values of electrical conductivity (CE) carried out along three S-N profiles perpendicular to the boundary with the Mediterranean Sea (Fig. 4; the profiles are those represented in Fig. 1).
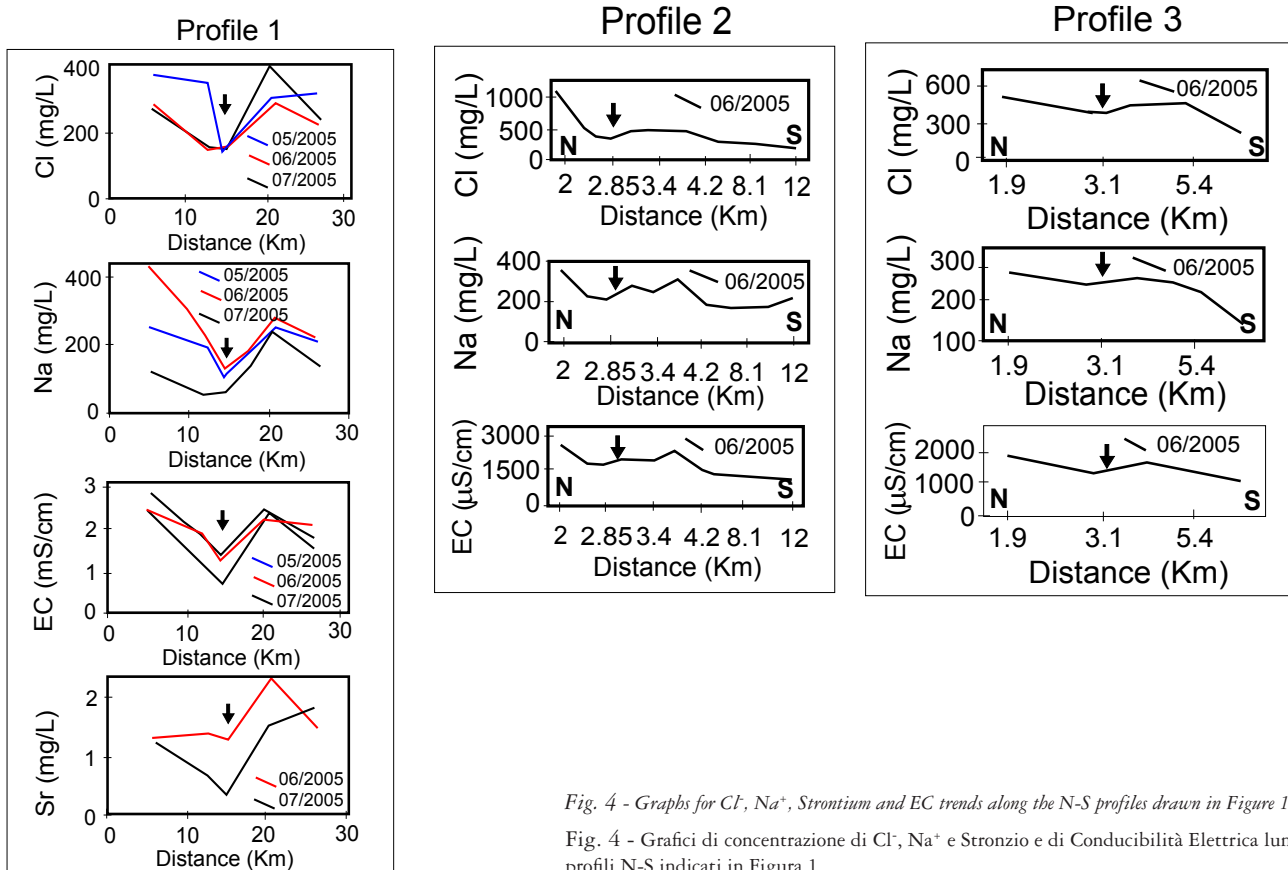

Fig. 4 - Graphs for Cl⁻, Na⁺, Strontium and EC trends along the N-S profiles drawn in Figure 1.

Fig. 4 - Grafici di concentrazione di Cl⁻, Na⁺ e Stronzio e di Conducibilità Elettrica lungo i profili N-S indicati in Figura 1.

The graphs of profile 1 show a drop in Cl⁻, Na⁺ concentrations and CE values in the first 15 kilometers from the coast. In this area, Cl⁻ values dropped from about 400 mg/L to less than 200 mg/L and Na⁺ values dropped from about 400 mg/L to less than 100 mg/L, while CE values decrease from almost 3000 to about 1000 µS/cm. Towards the South, the values raise again to reach higher contents for the various elements. The increase in strontium values may reflect the influence of evaporitic formations on the groundwater physico-chemical characteristics (Bougherira et al., 2015).

Profile 2 shows a decrease in the values of Cl⁻, Na⁺ and CE when moving away from the coast from a distance of about 2.85 km. However, unlike the first profile, no further increase occurs along the section. This is related to the absence of supply leaching from the evaporitic formations conveyed by the Seybouse.

The graphs of profile 3 are similar to those of profile 2. Average Cl⁻ concentration around 450 mg/L are observed up to 5.4 km from the coast. Concentrations drop sharply moving towards the South, probably for the same reasons as in the second profile.

Groundwater flow model

The model was calibrated in steady state conditions using the piezometric data collected in October 2003.

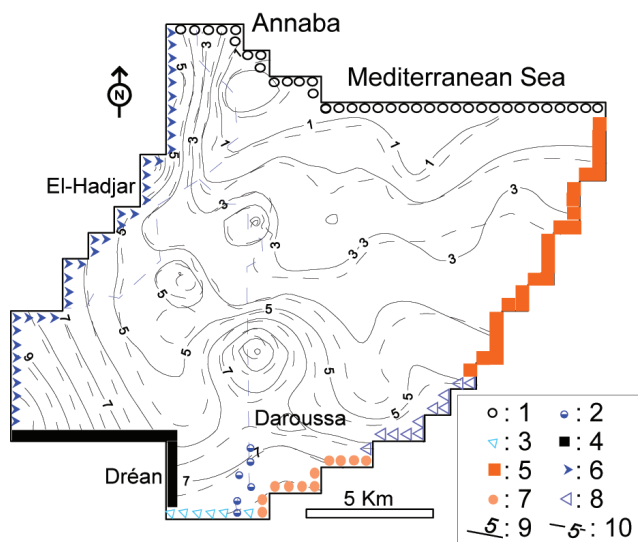The results for the deep gravel aquifer are showed in Figure 5.

Fig. 5 - Boundary Conditions and comparison between measured and calibrated piezometry for the deep gravel aquifer (steady-state conditions; reference year: 2003).
Legend: *Imposed Potential: 1. Sea, 2. Seybouse; No Flow Boundary: 3. High Level Alluvium and Numidian Clays, 4. Impermeable formations, 5. Ben-M'hidi Gaben limits; Fixed Head Boundary: 6. Metamorphic formations, 7. Alluvium Ancient, 8. Ben-M'hidi Graben limits; 9. Measured Piezometric Curve (values in m above mean sea level); 10. Simulated Piezometric Curve (values in m above mean sea level).*

Fig. 5 - Condizioni al contorno e confronto tra piezometria misurata e calibrata per l'acquifero ghiaioso profondo (condizioni stazionarie; anno di riferimento: 2003). **Legenda:** Potenziale Imposto: 1. Mare, 2. Seybouse; Flusso nullo: 3. Sedimenti alluvionali e argille Numidiane, 4. Formazioni impermeabili, 5. Graben Ben-M'hidi; Carico idraulico imposto: 6. Formazioni metamorfiche, 7. Sedimenti alluvionali, 8. Graben Ben-M'hidi; 9. Isopiezometriche misurate (valori in m sul livello medio del mare); 10. Isopiezometriche simulate (valori in m sul livello medio del mare).

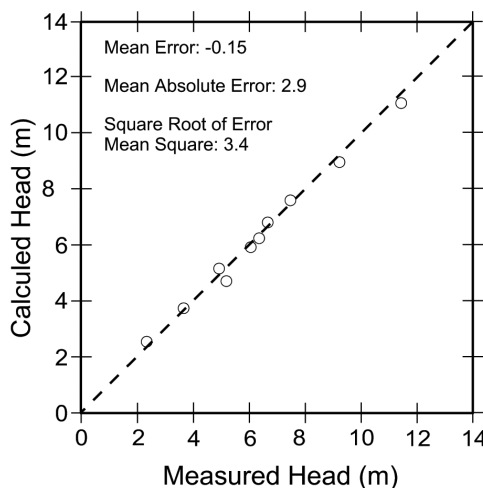The correspondence between the simulated and observed water heights is generally acceptable (Fig.6).

Fig. 6 - Comparison between measured and simulated piezometric head, October 2003 (values in m above mean sea level).

Fig. 6 - Confronto tra carico idraulico misurato e simulato, Ottobre 2003 (valori in m sul livello medio del mare).

To assess the effects of the increasing withdrawals on the aquifer, the model was run in transient conditions over a period of 12 years (2003-2015) (Fig.7 and Fig.8).

The groundwater flow model shows a significant drop in the piezometric levels due to the increase of the water withdrawals close to the coast.
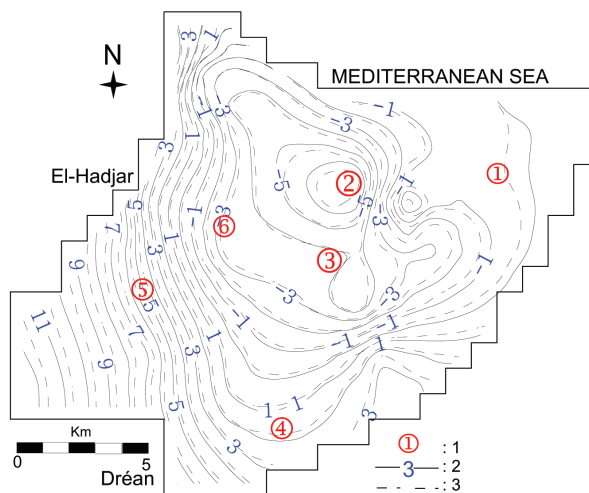

Fig. 7 - Comparison of reference and calibrated piezometry in transient conditions for the deep gravel aquifer (year 2015).
Legend: *1. Control Piezometers; 2. Measured Piezometric Curve (values in m above mean sea level); 3. Simulated Piezometric Curve (values in m above mean sea level).*

Fig. 7 - Confronto tra piezometria di riferimento e piezometria calibrata in condizioni transitorie per l'acquifero ghiaioso profondo (anno 2015).
Legenda: 1. Piezometri di monitoraggio; 2. Isopiezometriche misurate (valori in m sul livello medio del mare); 3. Isopiezometriche simulate (valori in m sul livello medio del mare).
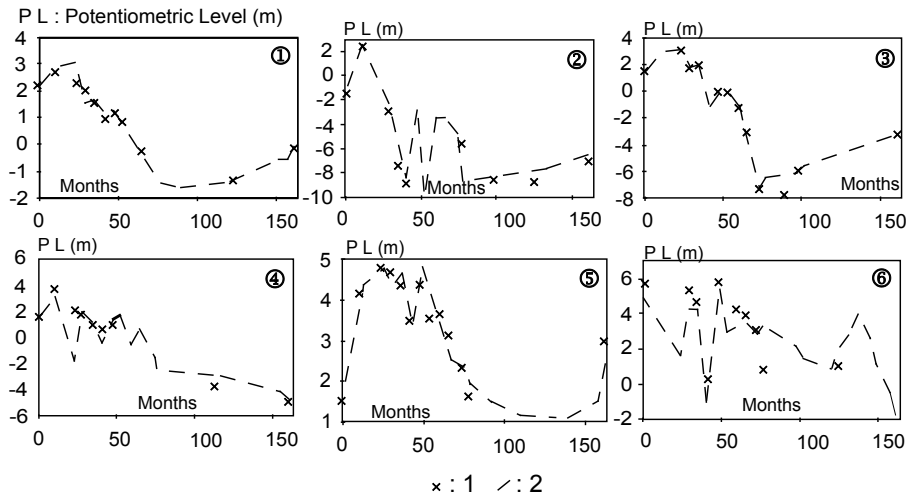
Fig. 8 - Transient model calibration (results at selected piezometers). Legend: 1. Observed Head (values in m above mean sea level); 2. Simulated Head (values in m above mean sea level).

Fig. 8 - Modello transitorio calibrato (risultati in corripondenza di piezometri selezionati). Legenda: 1. Carico idraulico osservato (valori in m sul livello medio del mare); 2. Carico idraulico simulato (valori in m sul livello medio del mare).
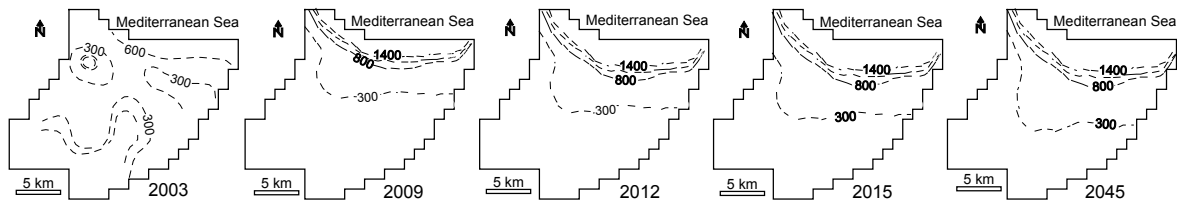

Fig. 9 - Simulations of marine intrusion in the lower Seybouse aquifer system (Cl⁻ concentration in mg/L).

Fig. 9 - Simulazioni del fenomeno di intrusione salina nel sistema acquifero di Seybouse (concentrazione di Cl⁻ in mg/L).

Figure 10 shows the hydraulic head and Cl⁻ concentration predicted in the aquifer by 2045.

The pumping rates would induce a decrease in the hydraulic heads up to –6 m with respect to the mean sea level and Cl⁻ concentrations higher that 10 g/L up to about 10 km from the coast.
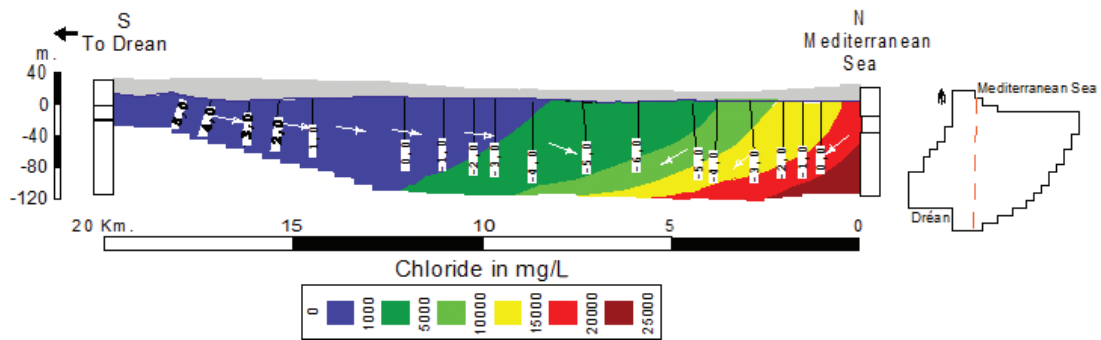

Fig. 10 - Cross section representative of the expected hydraulic head (values in m above mean sea level) and Cl⁻ concentration (values in mg/L) in the aquifer by 2045.

Fig. 10 - Sezione rappresentativa del carico idraulico atteso (valori in m sul livello medio del mare) e concentrazione di Cl⁻ (valori in mg/L) nell'acquifero entro il 2045.

Conclusions

This paper presented a numerical investigation of the seawater intrusion phenomenon in the Seybouse basin of Northeastern Algeria. The analysis of the physico-chemical parameters along three profiles perpendicular to the coast shows that the salinization of groundwater results from two main processes: the intrusion of seawater into the aquifer in the Northern part and the potential dissolution/precipitation of reservoir gypsum formations in the Southern part.

Numerical results show a significant drop in the groundwater levels close to the coast, due to increasing abstractions, and the advancing of saltwater inland.

Numerical predictions for 2045, considering an increase of withdrawals by 20%, show a fairly significant decrease in water levels, up to -6 m with respect to the mean sea level, and increase of Cl^- concentrations up to about 10 km inland.

These results show the necessity of adequate measures for the protection of the groundwater resources in the region, in order to meet the increasing demand for freshwater supply and to take into account the effects of climate change.

Competing interest
The authors declare no competing interest.

Author contributions
Samir Hani: collection data, numerical simulation and writting originaly draft. Fayçal Toumi: data processing and formal analysis. Nabil Bougherira: data processing and formal analysis. Isam Shahrour: supervision. Azzedine Hani: supervision.
All authors read and approved the final manuscript.

Additional information
Supplementary information is available for this paper at https://doi.org/10.7343/as-2023-635
Reprint and permission information are available writing to acquesotterranee@anipapozzi.it
Publisher's note Associazione Acque Sotterranee remains neutral with regard to jurisdictional claims in published maps and institutional affiliations.

REFERENCES

Acuña-Alonso, C., Fernandes, A.C.P., Álvarez, X., Valero, E., Pacheco, F.A.L., Varandas, S.D.G.P., Terêncio, D.P.S., & Fernandes, L.F.S. (2021). Water security and watershed management assessed through the modelling of hydrology and ecological integrity: A study in the Galicia-Costa (NW Spain). Science of The Total Environment, 759, 143905. https://doi.org/10.1016/j.scitotenv.2020.143905

AFNOR (French Association of Normalisation) (1987). Documentation: collection of french standards. 3rd ed. Bulletin of the libraries of France (BBF), 4, 386-388.

Alfio, M.R., Balacco, G., Parisi, A., Totaro, V., & Fidelibus, M.D. (2020). Drought Index as Indicator of Salinization of the Salento Aquifer (Southern Italy). Water, 12(7), 1927. https://doi.org/10.3390/w12071927

Bear, J. (1972). Dynamics of Fluids in Porous Media. New York, American Elsevier Pubishing Company, 764 pp.

Bouderbala, A. (2015). Groundwater salinization in semi-arid zones: an example from Nador plain (Tipaza, Algeria). Environmental Earth Sciences, 73(9), 5479-5496. https://doi.org/10.1007/s12665-014-3801-9

Bougherira, N., Hani, A., Toumi, F., Haied, N., & Djabri, L. (2015). Impact of ruban and industrial discharges on water quality in the Meboudja plain (Algéria). Hydrological Sciences Journal, 62(8), 1290-1300. https://doi.org/10.1080/02626667.2015.1052451

Chang, C.M., & Yeh, H.D. (2010). Spectral approach to seawater intrusion in heterogeneous coastal aquifers. Hydrology and Earth System Sciences, 14(5), 719-727. https://doi.org/10.5194/hess-14-719-2010

Cimino, A., Cosentino, C., Oieni, A., & Tranchina, L. (2008). A geophysical and geochemical approach for seawater intrusion assessment in the Acquedolci coastal aquifer (Northern Sicily). Environmental Geology, 55, 1473-1482. https://doi.org/10.1007/s00254-007-1097-8

Comte, J.C. (2008). Contribution of electrical tomography to modeling density flows in coastal aquifers. Application to three contrasting climatic contexts (Canada, New Calédonia, Sénégal). Doctoral thesis, Aix-Marseille Academy, Avignon and Vaucluse countries University, 198 p.

Datta, B., Vennalakanti, H., & Dhar, A. (2009). Modeling and control of saltwater intrusion in a coastal aquifer of Andhra Pradesh, India. Journal of hydro-environment Research, 3(3), 148-159. https://doi.org/10.1016/j.jher.2009.09.002

Grove, D.B., & Stollenwerk, K.G. (1984). Computer Model of One-Dimensional Equilibrium Controlled Sorption Processes. U.S. Geol. Survey Resources Investigations Report, 84, 4059.

Harbaugh, A.W. (2005). MODFLOW-2005, the U.S. Geological Survey Modular Ground Water Model the Ground-Water Flow Process. Reston, VA, USA: US Department of the Interior, US Geological Survey. Volume 6.

Ilias, S., & Pericles, L. (2016). Modeling seawater intrusion in overexploited aquifers in the absence of sufficient data: application to the aquifer of Nea Moudania, Northern Greece. Hydrogeology Journal, 24, 2123-2141. https://doi.org/10.1007/s10040-016-1455-2

INERIS. (2000). Underground Pollution: Parameters and parameterization of models in flow and transport of polluants. TRANSPORT Project, Program 2000.

Javandel, I., Doughty, C. & Tsang, C.F. (1984). Groundwater Transport: Handbook of Mathematical Models. American Geophysical Union, Water Resources Monograph, 10.

Lamouroux, C., & Hani, A. (2006). Identification of groundwater flow paths in complex aquifer systems. Hydrological Processes: An International Journal, 20(14), 2971-2987.

Lucassou, F., Schroëtter, J.M., Baptiste, J. & Coppo, N. (2019). Sensitivity of bretons coastal aquifers to saline intrusions. Final Report. BRGM/RP-69012-FR, 227.

Majour, H., Hani, A., & Djabri, L. (2018). Salinity and modelling of the Annaba aquifer system, North-East of Algeria. Journal of Water and Land Development, 37 (IV-VI). 113-120.

Mastrocicco, M. (2021). Studies on water resources salinization along the Italian coast: 30 years of work. Acque Sotterranee - Italian Journal of Groundwater, 10(4), 7-13. https://doi.org/10.7343/as-2021-537

Oude Essink, G.H.P. (2001). Saltwater intrusion in a three-dimensional groundwater system in the Netherlands: A numerical study. Transport in Porous Media, 43, 137-158.

Parisi, A., Alfio, M.R., Balacco, G., Güler, C., & Fidelibus, M.D. (2022). Analyzing spatial and temporal evolution of groundwater salinization through Multivariate Statistical Analysis and Hydrogeochemical Facies Evolution-Diagram. Science of the Total Environment, 862, 160697. https://doi.org/10.1016/j.scitotenv.2022.160697

Sae-Ju, J., Chotpantarat, S., & Thitimakorn, T. (2020). Hydrochemical, geophysical and multivariate statistical investigation of the seawater intrusion in the coastal aquifer at Phetchaburi Province, Thailand. Journal of Asian Earth Sciences, 191, 104165. https://doi.org/10.1016/j.jseaes.2019.104165

Sappa, G., Ferranti, F., & De Filippi, F.M. (2017). Assessment of Vulnerability To Seawater Intrusion For The Coastal Aquifer Of Dar Es Salaam (Tanzania). International Multidisciplinary Scientific GeoConference Surveying Geology and Mining Ecology Management, SGEM17 (12), 111-118.

Sappa, G, De Filippi, F.M., Ferranti, F, & Iacurto, S. (2019). Environmental issues and anthropic pressures in coastal aquifers: a case study in Southern Latium Region. Acque Sotterranee-Italian Journal of Groundwater, 8(1). https://doi.org/10.7343/as-2019-373

Vila, J.M. 1980. The Alpine chain of Eastern Algeria and Algerian–Tunisian borders. Doctoral thesis, Pierre and Marie-Curie University, Paris VI, France, 58-68.

Werner, A.D., Bakker, M., Post, V., Vandenbohede, A., Lu, C., Ataie-Ashtiani, B., Simmons, C., & Barry, D.A. (2013). Seawater intrusion processes, investigation and management: recent advances and future challenges. Advances in water resources, 51, 3-26. https://doi.org/10.1016/J.ADVWATRES.2012.03.004

Yang, J., Graf, T., Herold, M., & Ptak, T. (2013). Modelling the effects of tides and storm surges on coastal aquifers using a coupled surface-subsurface approach. Journal of contaminant hydrology, 149, 61-75. https://doi.org/10.1016/j.jconhyd.2013.03.002

Zheng, C., & Wang, P. (1999). MT3DMS: A Modular Three-dimensional Multispecies Transport Model for Simulation of Advection, Dispersion, and Chemical Reactions of Contaminants in Groundwater systems; documentation and user's guide. US Army engineer research and Development Center Contract reportSERDP-99-1, Vicksburg, Miss. http://hdl.handle.net/11681/4734

Zheng, C., Cao, G., Hill, M.C., & Ma, R. (2012). MT3DMS: Model use, calibration, and validation. American Society of Agricultural and Biological Engineers, 55(4), 1549-1559. DOI: 10.13031/2013.42263

Zouhri, L., Smaoui, H., Carlier, E., & Ouahsine, A. (2009). Modelling of hydrodispersive Processes in the fissured media by flux limiters schemes (Chalk aquifer, France). Mathematical and Computer Modelling, 50(3-4), 516-525. http://doi.org/10.1016//j.mcm.2009.0